

## Influence of Mining Thickness on the Rationality of Upward Mining in Coal Seam Group

Y. Li<sup>1\*</sup>, S. Zhang<sup>1</sup>, Z. Q. Yin<sup>2</sup>, W. R. Liu<sup>2</sup>, C. M. Li<sup>2</sup> and C. Wang<sup>3</sup>

<sup>1</sup>School of Resource and Safety Engineering, China University of Mining and Technology, Beijing, 100083, China

<sup>2</sup>The Provincial Key Laboratory of mining effects & disasters preventing under deep mining in Anhui, Anhui University of Science and Technology, Huainan, 232001, China

<sup>3</sup>Graduate School of Engineering, Nagasaki University, Nagasaki, 852-8521, Japan

Received 1 February 2016; Accepted 10 April 2016

### Abstract

This study aimed to determine the influence of mining thickness on the rationality of upward mining in coal seam group. Numerical simulation and theoretical analysis were performed to investigate the influence of the mining thicknesses of initial mining seam on the destruction and pressure relief effect of the upper coal seam in a high-gas coal seam group. The mechanical model of the roof failure based on the mining thickness was established by assuming that the gob formed after adjacent panels have fully been caved is the infinite plane. On the basis of this model, an equation was derived to calculate the roof failure height of the panel. Considering the geological conditions of No. 9 and No. 12 coal seams of Zhaogezhuang Coal Mine, economic effectiveness, and proposed techniques, we concluded that the top layer (4 m) of the No. 12 coal seam should be mined first. The top layer of the No. 9 coal seam should be subsequently mined. The top-caving technique was applied to the exploitation of the lower layer of the No. 12 coal seam. Practically monitored data revealed that the deformation and failure of the No. 2699 panel roadway was small and controllable, the amount of gas emission was reduced significantly, and the effect of upward mining was active. The results of this study provide theory basics for mine designing, and it is the provision of a reference for safe and efficient coal exploitation under similar conditions.

*Keywords:* Coal seam group, Upward mining, Initial mining thickness, Destruction influence, Pressure relief effect

### 1. Introduction

Chinese coal mines are applying downward mining in a coal seam group. When the occurrence of the lower coal seam is steady, the upper coal is called outburst coal seam, the roof is also not easily managed. If downward mining method is utilized, a series of security problems arises. Therefore, upward mining should be performed under these specific conditions. The lower coal seam should be used as a protective layer, and the upper coal seam should be exploited after pressure is fully relieved to achieve safe and highly efficient production [1], [2], [3], [4].

Upward mining is widely used as an effective method to prevent and control dynamic mining disasters regionally [5]. Many scholars investigated upward mining-related issues. Liu [6] demonstrated that lithology and mechanical stratum structure are important factors affecting upward mining and developed the ratio-value-criterion for upward mining, the "Three-Zone" judgment method, and the equation of rational interlayer spacing. Li and Qian [7] presented the balance theory of surrounding rocks to examine the mechanism of upward mining by considering that the safety spacing between two coal seams should be larger than the equilibrium height of surrounding rocks. Wang [8] analyzed the regulatory mechanism of overburden fracture evolution

in upward mining and the displacement and deformation regulation of the pressure-relief roadway. Wang [8] further discussed the mechanism and conditions of upward mining and argued that different lithologies between seams result in different ratio-value-criteria of upward mining. Also, Wang [8] modified and simplified the balance theory of surrounding rock. Sun [9] applied the surrounding rock equilibrium method, "Three-Zone" judgment method, and statistical analysis method to demonstrate the feasibility of upward mining. Jiang [10] used several methods to explore overburden movement, structural zoning characteristics, and upward pressure relief effect; Jiang [10] also established the evaluation method of the feasibility degree of upward mining. Qu and Zhang [11] simulated the upward pressure relief effect of difficult, deep, high-stress mining seam and concluded that upward pressure relief mining can significantly reduce the mining stress level of trouble coal seams with high stress. Previous studies mainly focused on the feasibility evaluation of upward mining, the movement regulation of overburden rock, and the specific mining thickness of particular scenarios. However, studies on the influence of mining thickness on the rationality of upward mining have yet to be performed. The initial mining thickness of the lower coal seam significantly influences the upper coal seam destruction and pressure relief effect, especially under the conditions with extra-thick coal seam group mining. Thus, reasonable coal mining sequence and thickness should be determined to release coal seam gas effectively and to maximize economic benefits [1], [12], and

\* E-mail address: liyang2026685@163.com

[13]. In this study, the above issues were thoroughly analyzed and discussed.

**2. General Information on the Project**

The occurrence of coal seam in Zhaogezhuang was stable and the geological structure was simple. Four minable coal seams have been identified. The No. 9 coal seam is a coal seam minable over the whole area. Its thickness was 1.47–10.49 m, with an average coal seam thickness of 4.10 m. Its hard roof was difficult to manage. The No. 9 coal seam was classified as a high-gassy outburst coal seam; this classification indicates that the coal seam can easily lead to dynamic disasters. The No. 11 coal seam was thin, with an average coal seam thickness of 1.12 m. The No. 12 coal seam was the main mining coal seam. Its thickness was 8.10–19.90 m, with an average thickness of 11.10 m. The No. 12 coal seam was distributed stably and was minable over the whole area. Its roof was composed of 8.0 m thick sandstone. The immediate roof consisted of 2.5 m thick muddy clay rock, and the roof joints were developed. Its direct bottom contained thin siltstone. The interlayer spacing of the No. 9 coal seam and the No. 12 coal seam was 31–43 m, with an average of 38 m.

The No. 9 coal seam was regarded as protective seam for mining because it was considered a high-gassy outburst coal seam. The No. 11 coal seam was only partly minable and could not function as protective seam. The No. 12 coal seam, an extra thick coal seam, remained stable. Selecting the No. 12 coal seam as the first mining coal seam could guarantee the annual output and produce the pressure relief effect on the No. 9 coal seam. This set up increased the breathability of the No. 9 coal seam, created conditions for gas release, and allowed secure and efficient coal exploitation.

**3. Theoretical Analysis of Coal Seam Group Upward Mining**

Upward mining sequence breaks the stress equilibrium state; as a result, internal stress rock redistribution, overburden deformation, and failure occur. Thus, mining-induced fractures are created. With the continued mining of the lower coal seam, fractures gradually develop in the upper coal seam; when the fractures reach a certain level, the shearing and deformation of the rock destroys the integrity of the coal seam and results in the unsuccessful implementation of upward mining [1]. Therefore, preventing the mutual sliding and stair-slip of the coal seam roof and further studying the overburden fracture evolution regulation are necessary to perform a successful upward mining and to achieve the desired effects.

**3.1 Zoning Characteristics of Overburden Failure**

According to the destruction level of overburden, applying the full caving method to manage the gob involves dividing the roof into caving zone, fracture zone, and curve subsidence zone from bottom to top [14], as shown in Figure 1.

The fracture zone is the zone where fractures develop after rock stratum fractures. The two main fracture types are: (1) the abscission fracture, which appears along the stratum and is mainly caused by unsynchronized bending because of large differences in mechanical nature between stratums; and (2) the vertical or oblique fracture, which is mainly caused

by rock stretching, shearing, and damaging [15]. According to the different rock fracture degrees and water-transmitting properties, fracture zones can generally be divided into the ‘strong fracture zone’ and the ‘weak fracture zone’. Strong fracture zone denotes that whole-thickness fractures exist in most of the rock with a certain interlayer slip, strata-dissecting fractures are well-developed and connected throughout the caving zone, and water transmitting ability is strong in this zone. In the upper weak fracture zone, rock stratum is mostly connected or rarely broken, has no dislocation between layers, exhibits poor connectivity between the fracture zones, and has poor water-transmitting ability.

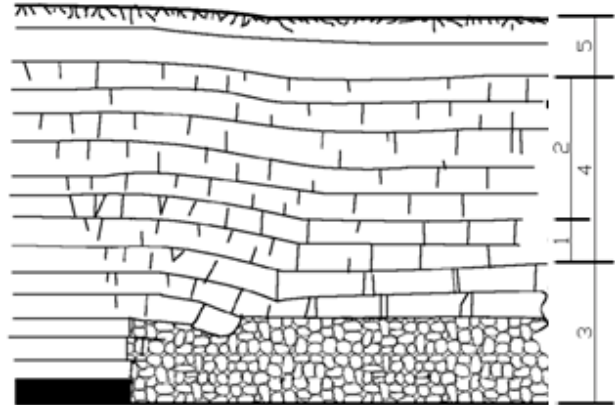


**Fig. 1** Damage zoning characteristics of overlying strata  
 Note: The damage zoning characteristics of overlying strata are listed. 1--strong fracture zone; 2--medium fracture zone; 3--caving zone; 4--fracture zone and 5--curve subsidence zone.

**3.2 Analysis of Mechanical Model for Panel Roof Failure Height**

The exploitation of the lower coal seam changes the overall mechanical environment of overlying strata and causes damage on the upper coal seam when upward mining is applied to the coal seam group. When the full caving method is employed to manage the roof of the long wall panel in the lower coal seam, its mining thickness is much less than its panel length, thus, it could be regarded as rectangular along the tilt direction. The present study abstracted the mining field as the mechanical model in Figure 2 because previous mechanical models of upward mining consider single panel conditions [16] and disregard the disturbance situation caused by the continuous mining of the lower coal seams.

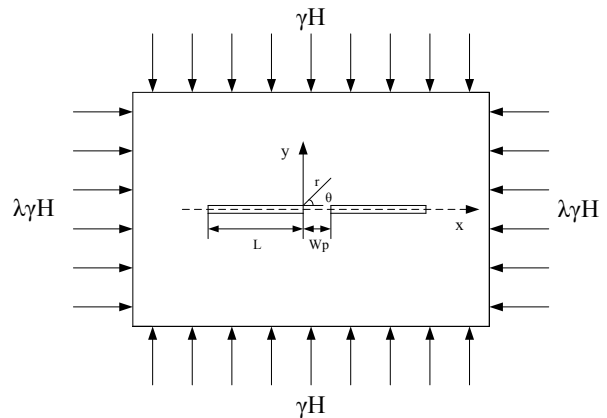


**Fig.2.** The calculating model of panel surrounding rock

Where  $L$  is the length of panel tendency, m.  $W_p$  is the pillar width, m.  $\gamma$  is the average volume-weight of the overlying strata,  $\text{kN/m}^3$ .  $H$  is the mining depth, m.  $\lambda$  is the horizontal pressure coefficient. Considering the mutual exploitation influence of adjacent panels, the roof stress distribution of panels is obtained [17]:

$$\begin{aligned}\sigma_x &= \frac{\gamma H}{2} \sqrt{\frac{2(L+W_p)}{\pi}} \operatorname{tg} \frac{\pi L}{2(L+W_p)} \cos \frac{\theta}{2} (1 - \sin \frac{\theta}{2} \sin \frac{3\theta}{2}) - \gamma H(1 - \lambda) \\ \sigma_y &= \frac{\gamma H}{2} \sqrt{\frac{2(L+W_p)}{\pi}} \operatorname{tg} \frac{\pi L}{2(L+W_p)} \cos \frac{\theta}{2} (1 + \sin \frac{\theta}{2} \sin \frac{3\theta}{2}) \\ \tau_{xy} &= \frac{\gamma H}{2} \sqrt{\frac{2(L+W_p)}{\pi}} \operatorname{tg} \frac{\pi L}{2(L+W_p)} \cos \frac{\theta}{2} \sin \frac{\theta}{2} \sin \frac{3\theta}{2}\end{aligned}\quad (1)$$

Considering the determined point  $(r, \theta)$  and the increasing the panel width  $L$ , we observed that the roof stress increases as the stress increases. In actual calculation,  $r < L$  and  $\lambda$  is regarded as 1; thus, roof stress can be expressed as follows:

$$\begin{aligned}\sigma_1 &= \frac{\gamma H}{2} \sqrt{\frac{2(L+W_p)}{\pi}} \operatorname{tg} \frac{\pi L}{2(L+W_p)} \cos \frac{\theta}{2} (1 + \sin \frac{\theta}{2}) \\ \sigma_2 &= \frac{\gamma H}{2} \sqrt{\frac{2(L+W_p)}{\pi}} \operatorname{tg} \frac{\pi L}{2(L+W_p)} \cos \frac{\theta}{2} (1 - \sin \frac{\theta}{2}) \\ \sigma_3 &= 0\end{aligned}\quad (2)$$

Assuming that the surrounding rock failure near the panel is in accordance with Mohr-Coulomb failure principle,

$$\sigma_1 - K\sigma_3 = R_c \quad (3)$$

We can substitute Eq. (2) in Eq. (3). Then, the boundary equation of the roof failure zone can be obtained:

$$r = \frac{\gamma^2 H^2 (L+W_p)}{2\pi R_c^2} \operatorname{tg} \frac{\pi L}{2(L+W_p)} \cos^2 \frac{\theta}{2} (1 + \sin \frac{\theta}{2})^2 \quad (4)$$

Therefore, the roof failure height  $h$  is expressed as follows:

$$h = r \sin \theta = \frac{\gamma^2 H^2 (L+W_p)}{2\pi R_c^2} \operatorname{tg} \frac{\pi L}{2(L+W_p)} \cos^2 \frac{\theta}{2} (1 + \sin \frac{\theta}{2})^2 \sin \theta \quad (5)$$

Calculating  $\frac{dh}{d\theta} = 0$ , we can obtain the roof failure height  $h_t$  in the state of plane stress:

$$h_t = \frac{1.57\gamma^2 H^2 (L+W_p)}{2\pi R_c^2} \operatorname{tg} \frac{\pi L}{2(L+W_p)} \quad (6)$$

The distance  $l_t$  between the roof failure height and the end of the panel can be determined:

$$l_t = \frac{0.42\gamma^2 H^2 (L+W_p)}{2\pi R_c^2} \operatorname{tg} \frac{\pi L}{2(L+W_p)} \quad (7)$$

The failure range in a plane strain state is smaller than that of a plane stress state. Thus, the failure range in plane strain state was not calculated. Not considering the plastic flow effect caused by yield stress leads to the increase in the failure range [18]. Therefore, engineering calculation should consider the influence of rock joint fracture. Using Eq. (6), we can determine the roof failure height  $h_\sigma$  of the panel:

$$h_\sigma = \frac{1.57\gamma^2 H^2 (L+W_p)}{2\pi \zeta^2 R_{mc}^2} \operatorname{tg} \frac{\pi L}{2(L+W_p)} \quad (8)$$

where  $\zeta$  is the influence coefficient of rock joint fracture and  $R_{mc}$  is the compressive strength of rock mass.

Gob contains a certain height in vertical direction. However, the failure height of the panel roof in the above equation only considers the horizontal scale and does not consider the mining height  $M$  of the lower coal seam and the caving zone height  $H_m$  of the lower rock strata. Therefore, the roof failure height  $h_\sigma$  can be modified as follows:

$$h_\sigma = \frac{1.57\gamma^2 (H - M - \frac{M - W}{(K - 1)\cos\alpha})^2 (L+W_p)}{2\pi \zeta^2 R_{mc}^2} \operatorname{tg} \frac{\pi L}{2(L+W_p)} + \frac{M - W}{(K - 1)\cos\alpha} \quad (9)$$

where  $\alpha$  is the coal seam dip angle, and  $W$  is the sinking value of the roof in the caving process.

Considering the mining effect of the lower coal seam, we observed that the overlying strata of gob experiences the generation and evolution of fractures, as well as macro-fracture forming and extending processes [19]. Within a certain height range above the caving zone, interlayer fractures can form. These interlayer fractures indicate strong fracture zones. Thus, the minor disturbances of coal seam in these zones could easily cause overall instability and larger stair dislocation. This scenario is unsafe for upward mining. Therefore, the adoption of upward mining sequence in the coal seam group depends on the location of the upper coal seam in the gob overlying strata. According to the damage zoning characteristics of the overlying strata, the vertical range in the overlying strata of the caving zone and the strong fracture zone is called the roof failure height  $h_\sigma$ . If the interlayer spacing of the upper and lower coal seams is larger than the roof failure height, the upper coal seam structure maintains integrity and continuity after disturbances occur; this condition is safe for upward mining.

## 4. Numerical Calculation Analysis

### 4.1 Numerical Calculation Models and Parameters

The present study uses the geological condition of Zhaogezhuang coal mine as the basis for analysis. The strata with small thickness and similar mechanical properties were grouped according to concrete rock features of the panel; a 3D numerical model of fast Lagrangian analysis of the continua was constructed. The model size (length, width and height) was confirmed as:  $380\text{m} \times 346\text{m} \times 300\text{m}$ , the number of units was 183084. Horizontal movement was limited at the side of the model, and vertical movement was limited at the bottom. The load on the top boundary was calculated with the weight of overburden. The Mohr-Coulomb model was adopted for the constitutive relation of the surrounding rock. The results were applied with theoretical calculation results for a comprehensive analysis. The three-dimensional model is shown in Figure 3.

### 4.2 Calculation Results and Discussion

For the mining condition of deep high-gassy coal seam group, the key to applying upward mining method is handling the relationship of three factors: interlayer spacing between the upper and the lower coal seams, mining thickness of the lower coal seam, and pressure relief effect. Considering the stability of the coal wall in large mining height, we calculated four plans to mine the upper layer of

the No. 12 coal seam: initial mining thickness at 2, 4, 6, and 11 m (full height).

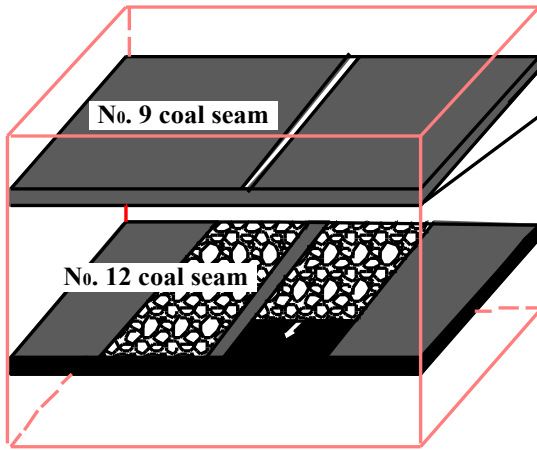


Fig.3. The exploitation of three-dimensional model

(1) The distribution characteristics of displacement field of the No. 9 coal seam

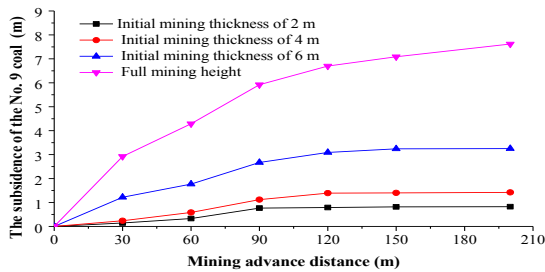


Fig.4. Subsidence curve of the No. 9 coal seam under different initial mining thickness

As the panel advanced, the sinking curve of the No. 9 coal seam was obtained by monitoring the vertical displacement of the No. 9 coal seam during numerical simulation. The central part of the No. 9 coal seam was selected as the monitoring point in the vertical direction, and the central part of the upper zone of the gob was selected as the monitoring point in the horizontal direction. Figure 4 presents the results.

As shown in Figure 4, the subsidence of the No. 9 coal seam increases with the panel advancing for the different initial mining thicknesses of the lower coal seam. However, the increase in subsidence slows down, especially when the initial mining thickness is 6 m or less. No changes occur when the panel advances to 120 m. When the initial mining thickness of the lower coal seam is 2 m and 4 m, the maximum subsidence value of the No. 9 coal seam after stabilization is 0.82 m and 1.42 m, respectively; the coal seam structure is complete. When the initial mining thickness is 6 m, the maximum displacement of the upper coal seam reaches 3.25 m and causes severe damage to the coal seam structure of the No. 9 coal seam. Thus, the different initial mining thicknesses of the lower coal seam produce different effects on the mechanical environment of surrounding rock of the protective layer of the No. 9 coal seam. Sufer 3D graphics software was applied to more intuitively show the stair sinking of the No. 9 coal seam when the neighboring panel advances by 200 m in the upper layer of the No. 12 coal seam at different mining heights and also to illustrate the vertical displacement distribution of the No. 9 coal seam; results are shown in Figure 5.

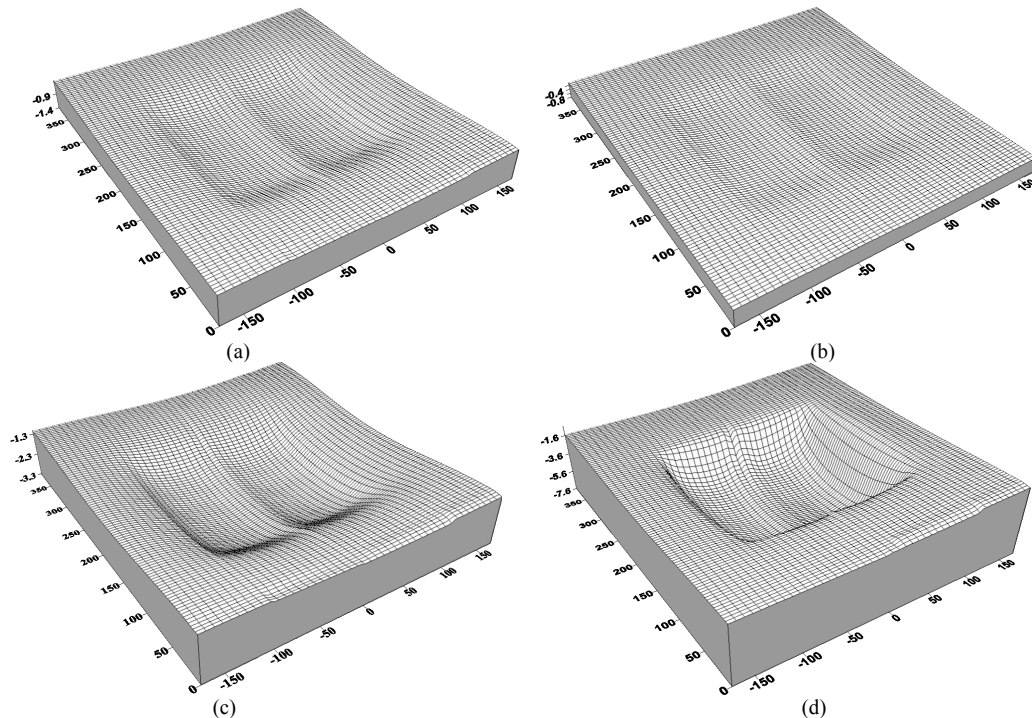


Fig.5. Displacement distribution map of the No. 9 coal seam under different initial mining thickness.

Note: figure (a) shows the data when the initial mining thickness of 2m; figure (b) shows the data when the initial mining thickness of 4m; figure (c) shows the data when the initial mining thickness of 6m; figure (d) shows the data when the initial mining thickness of 11m.

Figure 5 illustrates that as the initial mining thickness increases, the overburden subsidence movement intensifies, and the vertical displacement of the No. 9 coal seam also increases. When the initial mining thickness is 2 m, the effect of mining on the stair sinking of the upper No. 9 coal seam is not obvious; mining can be performed safely. When the initial mining thickness is 4 m, the maximum displacement value of the No. 9 coal seam reaches 1.42 m and dislocation caused by shearing occurs in the coal seam. However, the stair sinking value does not exceed half of its thickness. Thus, the integrity of the seam is good, and safe mining is possible after the lower coal seam becomes stable. When the initial mining thickness increases from 6 m to 11 m, the maximum displacement value of the upper coal seam increases from 3.25 m to 7.60 m, stair sinking phenomenon is quite serious, and the overall continuity is destroyed; under these conditions, the No. 9 coal seam cannot be mined.

(2) Distribution Characteristics of Stress Field of the No. 9 Coal Seam

When the lower protective layer is mined, the pressure-releasing rate of its upper protected coal seam can be calculated by Equation (10),

$$\eta = \sigma_z' / \sigma_z \tag{10}$$

In the equation,  $\eta$  is pressure relief rate;  $\sigma_z'$  is the vertical stress of coal seam after pressure releasing;  $\sigma_z$  is the initial vertical stress of coal seam.

Figure 6 shows the pressure relief rate changes of the No. 9 coal under different initial mining thickness:

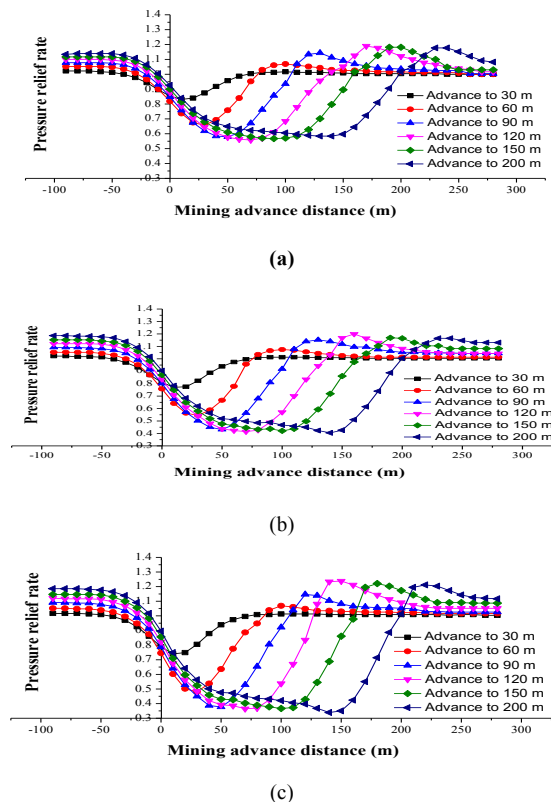


Fig.6. Pressure relief rate changes of the No. 9 coal under different initial mining thickness

Note: figure (a) shows the data when the initial mining thickness of 2m; figure (b) shows the data when the initial mining thickness of 4m; figure (c) shows the data when the initial mining thickness of 6m.

As shown in Figure 6, when the initial mining thickness of the No. 12 coal seam is 2 m, the average pressure relief rate of the No. 9 coal seam is about 0.6; this pressure relief effect is not ideal. When the initial mining thickness reaches 4 and 6 m, the average pressure relief rates are 0.4 and 0.35, respectively; the pressure-relief effect is enhanced. Figure 6 also shows that as the panel advances in the lower coal seam, the vertical stress of the protected layer located above the gob decreases significantly compared with the original stress; the pressure relief rate decreases with the increasing of the initial mining thickness. This is mainly because mining makes overburden strata of the gob deformity and the stress is released. As the initial mining thickness increases, the fracture range of the overburden strata of the gob increases; the pressure relief effect is also enhanced, and this effect creates conditions for the desorbing and flowing of pressure relief gas. Gas flows from high pressure areas to low pressure areas under its pressure gradient, and part of the gas can flow into the protective layer through the mine ventilation system and then out to ground level; the purpose of upward pressure relief mining is eventually realized.

The simulated mining of the No. 9 coal seam using four conditions of initial mining thicknesses of 2, 4, 6, and 11 m was performed to determine the reasonable upward mining in coal seam group. When the mining thickness of the upper layer of the No. 12 coal seam is 2 m or 4 m, overburden strata failure is not serious, and the stair dislocation effect is also not significant; these conditions satisfy the requirements of upward mining. Considering the high gas occurrence condition of the No. 9 coal seam, when the mining thickness of the upper layer of the No. 12 coal seam is 2 m, the pressure relief effect isn't ideal. Therefore, the most reasonable mining procedure simulated is to first mine the 4 m upper layer of the No. 12 coal seam and then mine the No. 9 coal seam after pressure is relieved.

5. Project Practice

The No. 2699 panel depth of Zhaogezhuang coal mine is 900 m, the dip angle is 28°, the average volume-weight of the overlying strata  $\gamma$  is 25 kN/m<sup>3</sup>, residual expansion coefficient K is 1.25, sinking value of the roof during caving process is 0.2 m, the influence coefficient of rock joint fracture  $\zeta$  is 0.9. Interlayer lithology is mainly sandstone, which was classified into hard rock, the average compressive strength is 56 MPa, the tilt length of designing panel L is 90 m, and the coal pillar width is 29 m. The above parameters were substituted into the formula to obtain the roof failure height and then combined with the numerical simulation. Analysis results of the rationality of different mining methods of the No. 12 coal seam are shown in Table 1.

If the existing installations and economic benefits are considered, mining the 6 m upper layer of the No. 12 coal seam is economically unreasonable, because this mining operation would require the introduction of new technology and equipment despite being a mine with only small reserves. Our comprehensive analysis demonstrated that mining at 4 m of the upper layer of the No. 12 coal seam should be initially performed. Then, the No. 9 coal seam should be mined after pressure is relieved. Finally, top caving should be applied to mine the lower layer of the No. 12 coal seam.

**Table 1.** Rationality analysis of the No.12 coal under different mining methods

Influence Condition		Initial Mining Thickness of 2m	Initial Mining Thickness of 4m	Initial Mining Thickness of 6m	Full Thickness (11m)
Upward mining discrimination	Roof failure height/m	20.4	30.2	38.7	>>38.0
	Whether meet the conditions	Yes	Yes	No	No
Gas impact	The effect of pressure relief	Medium	Good	Good	Good
Technical conditions	Whether meet the equipment requirements	Yes	Yes	No	No
Conclusion		Unreasonable	Reasonable	Unreasonable	Unreasonable

According to the field practice of the No. 2699 panel, fully mechanized mining was adopted to mine the 4 m upper layer of the No. 12 coal seam. The integrity of the No. 9 coal seam was better, and the failure was not serious. The overall sinking of the roadway was not obvious, but the gas emission decreased significantly. Through the systematical arrangement of mine pressure observation data, the surface displacement and deformation rate curve of the surrounding rock of roadways over time were obtained, as shown in Figure 7.

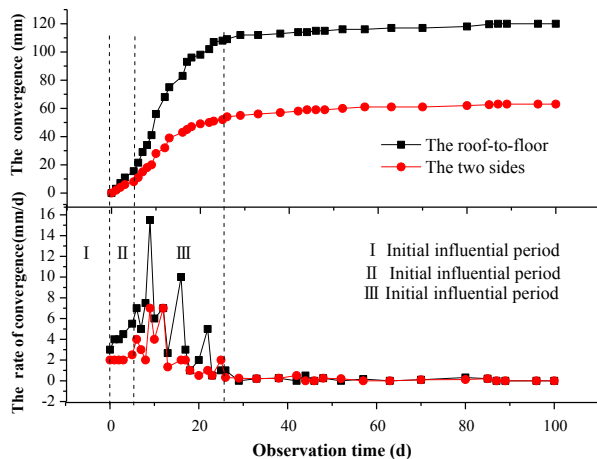


**Fig.7.** Surface displacement of the surrounding rock deformation curve varying with time

Figure 7 shows that the surface displacement of the surrounding rock of roadway is divided into initial influential period, strong influential period, and influential recession period. In the initial influential period, the roof-to-floor cumulative convergence is 21 mm, the maximum rate of roof-to-floor convergence is 4.5 mm/d, the convergence at the two sides is 10 mm, and the maximum rate of convergence at the two sides is 2.5 mm/d. In the strong influential period, the roof-to-floor cumulative convergence is 105 mm, the maximum rate of roof-to-floor convergence is 15.5 mm/d, the convergence at the two sides is 50 mm, and the maximum rate of convergence at the two sides is 7 mm/d. The roadway remains stable in the influential recession period. The total roof-to-floor cumulative convergence is 120 mm and the total convergence at the two sides is 63 mm. The effects of the deformation and failure of

roadway are small and controllable. These findings confirmed our theoretical analysis and numerical results.

## 6. Conclusion

In this study, the mechanical model of the roof failure based on the mining thickness effect was established. The roof failure height formula was also derived. The theoretical basis for the rationality of upward mining analysis was also provided.

Simulation mining at 2, 4, 6, and 11 m (full height) of the upper layer of the No. 12 coal seam showed the following: At 2 and 4 m of the upper layer, the requirements of upward mining can be satisfied. At 2 m initial mining thickness of the No. 12 coal seam, the pressure relief effect was not ideal. At  $\geq 4$  m initial mining thickness, the pressure relief effect was enhanced and conditions for gas absorption and flow were established. Considering the theoretical analysis results and the economic benefit of coal mining, we concluded that mining at 4 m of the upper layer of the No. 12 coal seam should be initially performed; then, the No. 9 coal seam should be mined after pressure is relieved. Finally, top caving should be applied to mine the lower layer of the No. 12 coal seam.

Field practice demonstrated that the surrounding rock movement of the No. 2699 panel roadway was divided into initial influential period, strong influential period, and influential recession period. The effects of deformation and failure were small and controllable. The roadway gas emission was significantly reduced. The effect of upward mining was active.

Our research provided a theoretical basis for the mining design of coal mines and for the safe and efficient coal exploitation under similar conditions.

## Acknowledgements

This work was supported by the National Key Basic Research Program of China No.2014CB260403, the National Natural Science Foundation of China No.51504005, No.51304007, the University Science Research Project of Anhui Province No.KJ2015A091 and Open Foundation of Anhui Province Key Laboratory of Deep Coal Mine Excavation Response & Disaster Prevention and Control No.KLDCMERDPC14105.

## References

- Zhang, Y., Liu, C. A., Zhang, X. B., Liu, K. M., Zhang, S. K., Zhao, G.P., "The influence of ascending mining on the movement character of overlying coal seam in coal seams group", *Journal of China Coal Society*, 36(12), 2011, pp. 1990-1995.
- Jiang, Y. D., Meng, L., Zhao, Y. X., Pan, L., Lei, Y., "The Feasibility Research on Ascending Mining under the Condition of Multi-Disturbances ", *Procedia Environmental Sciences*, 12, 2012, pp. 758-764.

3. Tang, J. X., Li, Y. L., Jia, Y. L., Sun, L. L., "Study on zoning of overburden strata and roadway deformation of ascending mining in thin coal seam", *Advance Materials Research*, 616-618, 2012, pp. 505-509.
4. Han, J., Zhang, H. W., Zhang, P. T., Zhang, J., Li, M., "Over mining in Kailuan, China mining area", *Proceedings of the 28th International Conference on Ground Control in Mining, Morgantown, WV*, 2009, pp. 305-311 .
5. Liang, S., Li, X., Mao, Y., Li, C., "Time-domain characteristics of overlying strata failure under condition of longwall ascending mining", *International Journal of Rock Mechanics and Mining Sciences*, 23(2), 2013, pp. 207-211.
6. Liu T. Q., "The possibility of using the upward mining method", *Journal of China Coal Society*, (1), 1981, pp. 18-29.
7. Li H. C., Qian, M. G., "A study of ascending mining method at Kongzhuang mine", *Journal of China University of Mining and Technology*, (2), 1982, pp. 11-23.
8. Wang L. Q., LI Z. H., "Technique of ascending mining in coal seams", Beijing: China Coal Industry Publishing House, 1995. China, pp.3-20.
9. Song, G. J., Wang, Y. L., "Upward mining to improve complex roof control of seam", *Coal Science and Technology*, 32(5), 2004, pp. 15-18.
10. Jiang, J. Q., Sun, C. J., Yin, Z. D., Zhang, D. Z., "Study and practice of bottom slicing relieving mining in condition of trouble coal seams with high ground stress under deep coal mine", *Journal of China Coal Society*, 29(1), 2004, pp. 1-6.
11. Qu, H., Zhang, D. Z., "Numerical simulation on ascending mining method of complicated coal seam in deep mine", *Ground Pressure and Strata Control*, 21(4), 2004, pp. 56-58.
12. Xie, H. P., Chen, Z. H., Wang, J. C., "Three dimensional numerical analysis of deformation and failure during top coal caving", *International Journal of Rock Mechanics and Mining Sciences*, 36(5), 1999, pp. 661-670.
13. Lan, T. W., Zhang, H. W., Li, S., Han, J., Song, W. H., Batugin, A. C., Tang, G. S., "Numerical study on 4-1 coal seam of Xiaoming mine in ascending mining", *The Scientific World Journal*, 2015, Article ID 516095, 4 pages, doi:10.1155/2015/516095.
14. Qian, M. G., Shi, P. W., "Mine pressure and ground control", Xuzhou: China University of Mining and Technology Press, 2003. China, pp.65-96.
15. Wang, C., Zhang, N., Han, Y., Xiong, Z., Qian, D., "Experiment research on overburden mining-induced fracture evolution and its fractal characteristics in ascending mining", *Arabian Journal of Geosciences*, 8(1), 2013, pp. 13-21.
16. Zhang, J. C., Zhang, Y. Z., Liu, T. Q., "Rock mass permeability and coal mine water inrush", Beijing: Geological Publishing House, 1997, pp. 24-29.
17. Wu, J. L., "Elasticity", Beijing: Higher Education Press, 2001. China, pp.98-105.
18. Feng G. R., Wang, X. X., Kang, L. X., "A probe into "Mining Technique in the Condition of Floor Failure" for coal seam above long wall goafs", *Journal of Coal Science and Engineering*, 14(1), 2008, pp. 19-23.
19. Khare, S., Rao, Y. V., Murthy, C. SN., Vardhan, H., "Multiple seam mining a critical review *Journal of mines*", *Metals and Fuels*, 54(12), 2006, pp. 327-329.